

# Radio-upgradation of the GRAPES-3 experiment with the beam-forming approach.

---

**Subhadip Saha,<sup>a,b,\*</sup> Pankaj Jain,<sup>a</sup> Tim Huege,<sup>b,c</sup> Dave Z. Besson<sup>d</sup> and Sara Martinelli<sup>b,e</sup>**

<sup>a</sup>*Indian Institute of Technology Kanpur, Kanpur, UP-208016, India*

<sup>b</sup>*Institut für Astroteilchenphysik, Karlsruhe Institute of Technology (KIT), P.O. Box 3640, 76021 Karlsruhe, Germany*

<sup>c</sup>*Vrije Universiteit Brussel, Astrophysical Institute, Pleinlaan 2, 1050 Brussels, Belgium*

<sup>d</sup>*Department of Physics and Astronomy, University of Kansas, Lawrence, KS 66045, USA*

<sup>e</sup>*Instituto de Tecnologías en Detección y Astropartículas (CNEA, CONICET, UNSAM), Buenos Aires, Argentina*

*E-mail:* [subhadip.phy@gmail.com](mailto:subhadip.phy@gmail.com), [sahas@iitk.ac.in](mailto:sahas@iitk.ac.in)

The GRAPES-3 (Gamma Ray Astronomy PeV EnergieS phase-3) is a globally recognized experiment that detects cosmic rays roughly over  $10^{13}$  eV to  $10^{16}$  eV. It has an excellent core-resolution at PeV energies. We are planning for a radio-extension to the GRAPES-3 experiment and designing an array with 60-70 antennas. The array has been envisaged to work on the beam-forming approach to detect cosmic rays over the PeV energy range. We have used the beam-forming framework to optimize the design of our radio array. With the beam-forming technique, we are endeavoring to lower the radio-detection threshold down to few tens of PeV. Using CoREAS simulations, we have been able to demonstrate the detection of 10 PeV air-shower events, at the  $4\sigma$  detection threshold. This may enhance the overall detection threshold of the GRAPES-3 experiment.

## 1. Introduction

Short radio frequency (RF) pulses with lengths of nanoseconds (ns) are emitted from cosmic ray induced air showers which can be recorded with an array of antennas as demonstrated at the LOPES, CODALEMA, Tunka-Rex, LOFAR, and AERA observatories for energies typically 100 PeV and above. Below 100 PeV, strength of the induced signal starts falling beneath the overwhelming background noise, hence the detection becomes gradually more challenging. We aim to address these technical challenges with sophisticated beam-forming (BF) techniques to lower the radio-detection (RD) threshold. We are planning for a radio-upgradation of the GRAPES-3 experiment with the implementation of the near-field BF-approach [1, 2]. We are designing a radio array with 60-70 antennas, envisaged to function along with the existing array of scintillator detectors (SDs), to detect cosmic rays over the PeV energy range. The SD-array will primarily provide external triggering to the RD-framework and reconstruct the core and axis of the air-shower. It has an excellent core-reconstruction resolution, approximately 0.5 m at 1 PeV. Therefore, the SD-array will complement the BF-framework and aid in the reconstruction of some of the essential shower parameters. With the BF-approach, we endeavor to lower the RD-threshold to as low as possible. We have been using this BF-framework to optimize the design of our radio-array. The advent of the radio-detection facility at the GRAPES-3, may also enhance its upper detection threshold.

We have used CoREAS [3] simulations to determine typical radio signals, at the altitude (i.e., 2200 m) and location of the GRAPES-3 experiment. The developed BF-framework can be adapted to different experiments.

## 2. Technical details

We have used the beam-forming (“radio-interferometric technique”) functionality within the NuRadioReco [4] framework for the entire analysis and optimization studies. We have primarily focused on maximizing the signal-to-noise ratio (SNR) and the detection efficiency. The SNR is defined as the ratio of the root mean square (RMS) of the signal over 10 ns, around the peak, and the RMS of the noise portion of the trace. The detection efficiency represents the proportion of events with SNR 4.0 and above, after beamforming.

The performance of beam-forming depends on several factors related to the array-geometry, i.e., the distribution of antennas and antenna-clusters and is directly impacted by the design. A cluster of antennas is referred as a station. Some of the important parameters are the spacing between the adjacent antennas, i.e., the inter-element spacing ( $d_{\text{ANT}}$ ), total number of stations ( $N_{\text{ST}}$ ), number of antennas ( $n_{\text{ANT}}$ ) in an individual station, total number of antennas ( $N_{\text{ANT}}$ ), distance between antenna mini-clusters (i.e., smaller sub-arrays or sub-stations), i.e., the inter-sub-array spacing or inter-sub-station spacing ( $d_{\text{ST}}$ ), distance between stations or antenna-clusters (larger), i.e., the inter-station spacing ( $D_{\text{ST}}$ ) and so on. Some of these parameters are correlated. We have probed these parameters and monitored the performance outcome.

We have compared the BF-performance for different array-geometries to estimate the optimal array-layout and dimensions. We have chosen the hexagonal layout for the base-station as it provides compact and uniform sampling. Besides a single large station, we have also considered a distributed configuration of antennas in smaller sub-arrays or sub-stations and compared their performances.

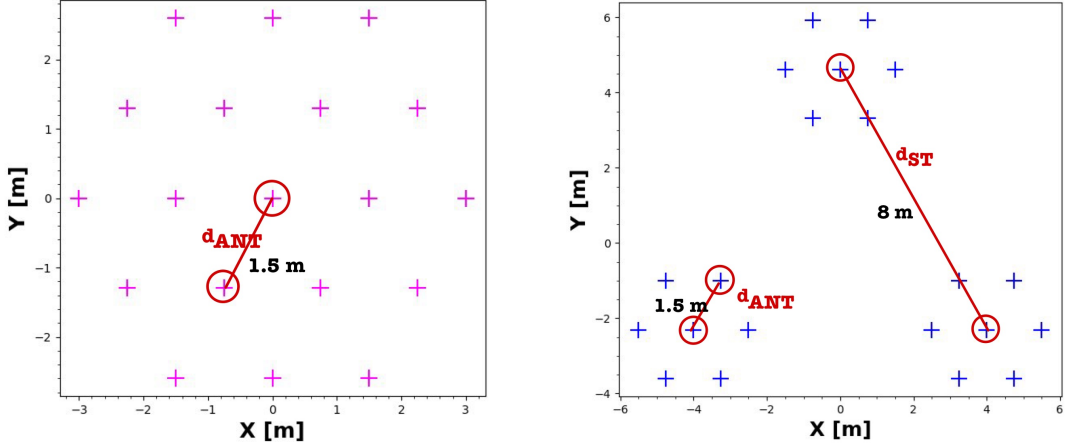


**Figure 1:** Two different array-geometries. The left profile depicts the array-layout for a SA-station. The right profile depicts typical array-layout for a DA-station. Each of the magenta and blue markers represents location of a dual-polarized SKALA-2.1 antenna [5].

A typical comparison is made between the array-geometries in Figure 1. The array layout on the left side in Figure 1, is referred as a single-array (SA) station which is a "single" large regular array. The array layout on the right side in Figure 1, is referred as typical a distributed-array (DA) station, in which the antennas are distributed in 3 smaller sub-arrays or sub-stations. We have found that the DA-geometry has a better SNR and detection efficiency than the SA-geometry, hence we selected it as the base-array. The base-array is the building block for the larger array which has been envisaged with 60-70 antennas.

We have chosen a typical value for  $d_{ANT}$  of 1.5 m, for reference, the wavelength at 150 MHz is 2 m. For comparison, the SKA-Low array has a mean inter-antenna spacing of 1.35 m. At low frequencies, where the wavelength is longer than this distance, there will be mutual coupling among the antennas, which has not been considered in this study. Next, we have compared the performance of three different configurations of the DA-geometry with  $d_{ST}$  values of 8 m (Type-1), 16 m (Type-2), and 24 m (Type-3), respectively. This provides insight about the optimal value of  $d_{ST}$ , one of the important parameters in our optimization. Likewise, we have increased the number of antennas ( $N_{ANT}$ ) and varied  $D_{ST}$  to estimate the optimal values and finalized the layout of the complete array.

In this report, we are presenting results only for 10 PeV showers for three different primaries, which are Protons, Helium and Iron nuclei. With CoREAS, we have simulated the expected radio emission from extensive air showers. The data-set contains showers for 6 different zenith angles, which are  $0^\circ$ ,  $10^\circ$ ,  $20^\circ$ ,  $30^\circ$ ,  $40^\circ$ , and  $50^\circ$ . The azimuth angle has been varied from  $-180^\circ$  to  $180^\circ$  in intervals of  $10^\circ$  for each simulation. The findings are valid over an area of radius 75 m from the shower core. The signal-traces have been processed through the detector response in NuRadioReco which primarily includes frequency and directional response of the SKALA-2.1 antenna [5]. The radio interferometric technique (RIT) functionality [1, 2], available in NuRadioReco, has been adapted for the expected noise level, signal strength, frequency bands and array layouts.

Galactic background noise and instrumental noise have been added to the band-passed signal to simulate a realistic signal processing chain. The diffused galactic radio background noise has been simulated, from the radio background data [6, 7], with the PyGDSM package. The instrumental noise is drawn from the Rayleigh distribution, with a RMS value of 6 microvolts, which is equivalent to a receiver noise temperature of 160 K at an impedance of  $100\ \Omega$  or a noise temperature of 330 K at an impedance of  $50\ \Omega$ . The typical receiver temperature is around 50-60 K, for the SKALA antennas.

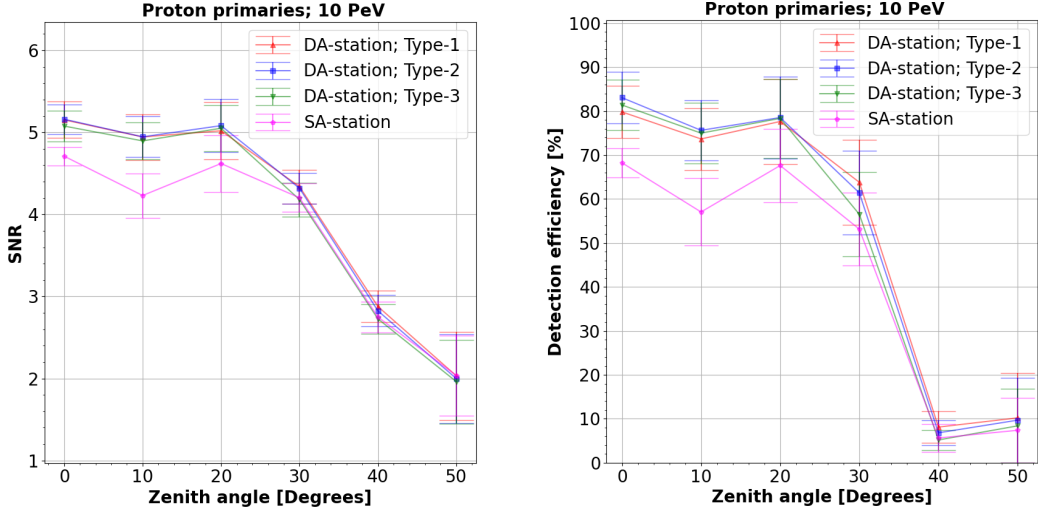


**Figure 2:** Variation of the SNR (Left) and the detection efficiency (Right) with zenith angle, for 4 different array-layouts. This is for proton primaries.

### 3. Results

#### 3.1 The base-array geometry

Here we have compared the performance of the SA-station and 3 “Types” of the DA-stations with the BF-approach. Each configuration represents a different inter-sub-station spacing ( $d_{ST}$ ). Type-1, Type-2, and Type-3 have separations of 8 m, 16 m, and 24 m, respectively. In Figure 2, Figure 3, and Figure 4, the variation of SNR and detection efficiency with zenith angle have been shown, for SA-station and DA-stations, for Proton, Helium, and Iron primaries, respectively. We can see that the DA-geometry has better SNR and detection efficiency compared to the SA-geometry. Therefore, the DA-geometry has been promoted as the base-array geometry. The performance of the DA-stations for 3 different configurations is roughly comparable for proton and helium primaries, in the 100-200 MHz frequency band, which is an optimal band. However, in the case of iron primaries, we note a notable drop in performance of the Type-3 DA-station which indicates that 24 m separation is not an optimal dimension. This is probably because for iron primaries, more energy goes into muons, hence less energy goes into the electromagnetic cascade. Also, for heavier primaries, the  $X_{max}$  is at higher altitude and the signal is comparatively more diffuse, hence

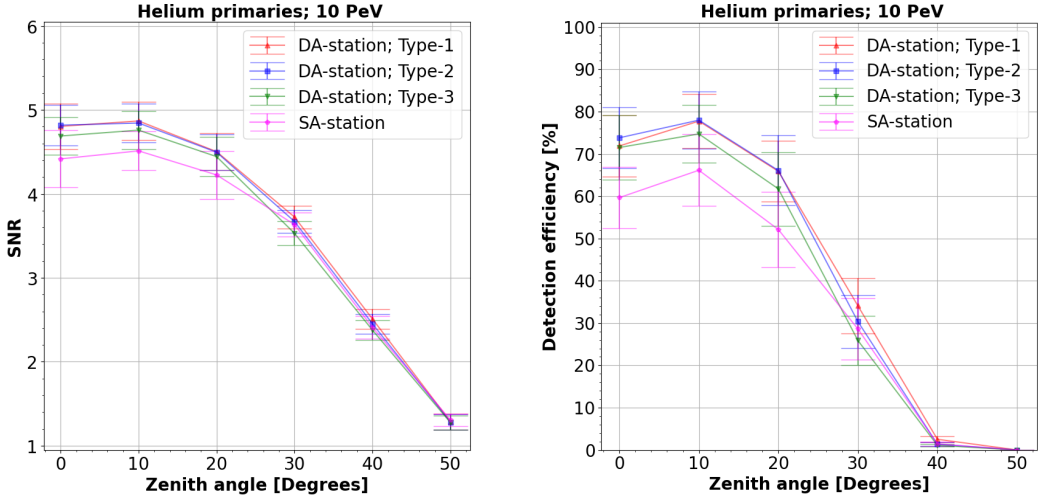


**Figure 3:** Variation of the SNR (Left) and the detection efficiency (Right) with zenith angle, for 4 different array-layouts. This is for helium primaries.

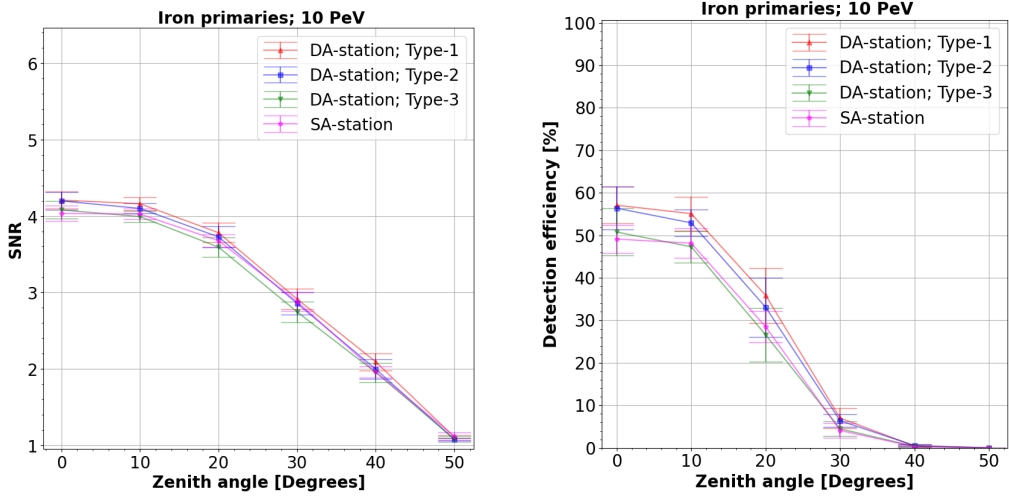


**Figure 4:** Variation of the SNR (Left) and the detection efficiency (Right) with zenith angle, for 4 different array-layouts. This is for iron primaries. We note that the performance of the "Type-3" DA-station drops off notably.

comparatively lower signal strength. Even for the helium primaries, the performance of the Type-3 DA-stations is comparatively lower than the other 2 "Types". Therefore, we chose to rule this out from further analysis. The optimal value of  $d_{ST}$  is in the range of 8-16 m.

### 3.2 Extension of the array

We next consider an extension of the array layout by increasing number of stations ( $N_{ST}$ ), i.e., by simply repeating the base-station. We would first double the number of antennas ( $N_{ANT}$ ),

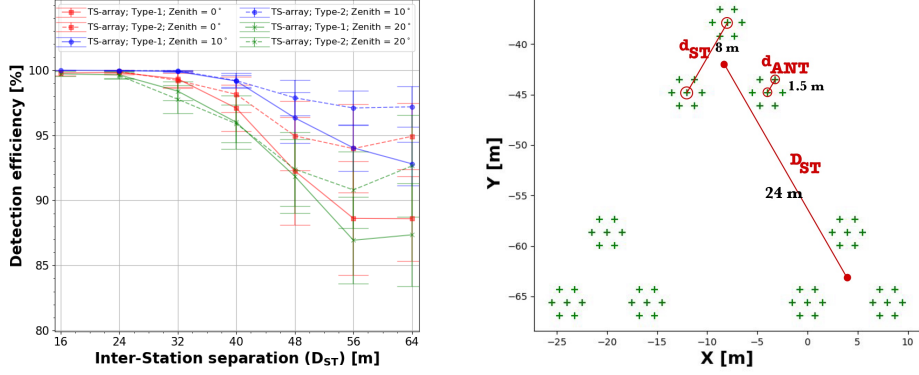


**Figure 5:** The Left profile depicts variation of the detection efficiency of the TS-arrays with the variation in the inter-station separation ( $D_{ST}$ ). This is for 10 PeV Iron showers, for zenith angles  $0^\circ$ ,  $10^\circ$ , and  $20^\circ$ . The Right diagram shows a typical TS-array. Each of the markers represents a dual-polarized SKALA antenna.

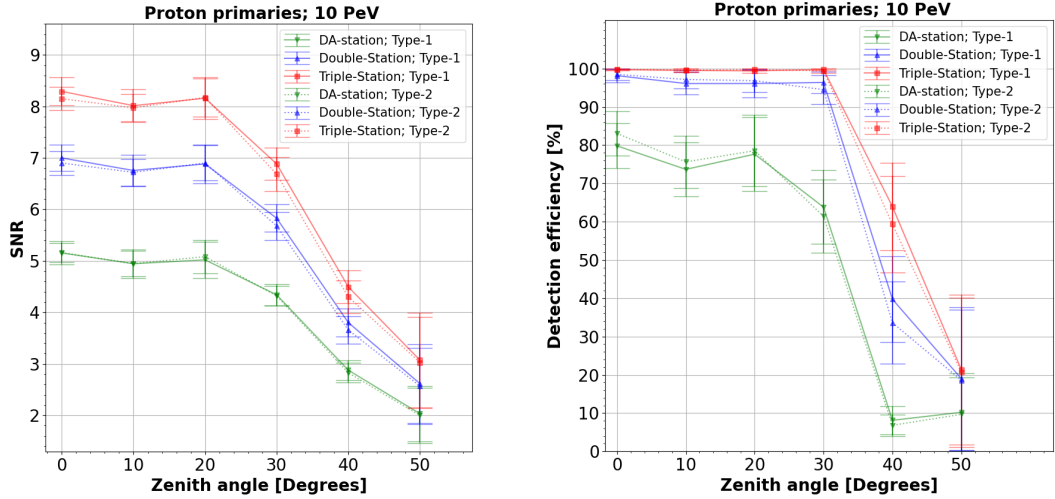


**Figure 6:** Left Profile presents the SNR-variation with increasing number of antennas. Right Profile presents variation of the detection efficiency with increasing number of antennas. The Green curve is for the DA-stations with 21 antennas. The Blue curve is for the double-stations with 42 antennas and the Red curve is for the triple-stations with 63 antennas. The solid curves are for the Type-1 base-stations and the dashed curves are for the Type-2 base-stations.

i.e., 2 DA-stations, to be referred to as a “Double-Station” (DS) and then add another DA-station to construct a “Triple-Station” (TS) and compare their performances. The distance between the centers of two DA-stations, is the inter-station spacing ( $D_{ST}$ ). In a TS-array, three DA-stations are placed such that the centers of the DA-station are on the vertices of an equilateral triangle. In other words, the distance between the DA-stations (i.e.,  $D_{ST}$ ) is equal and on a triangular layout.

In the left profile of Figure 5, it is shown how the detection efficiency of the TS-arrays typically drops with  $D_{ST}$  after 24 m, for iron showers at zenith angles  $0^\circ$ ,  $10^\circ$ , and  $20^\circ$ . Therefore, the optimal

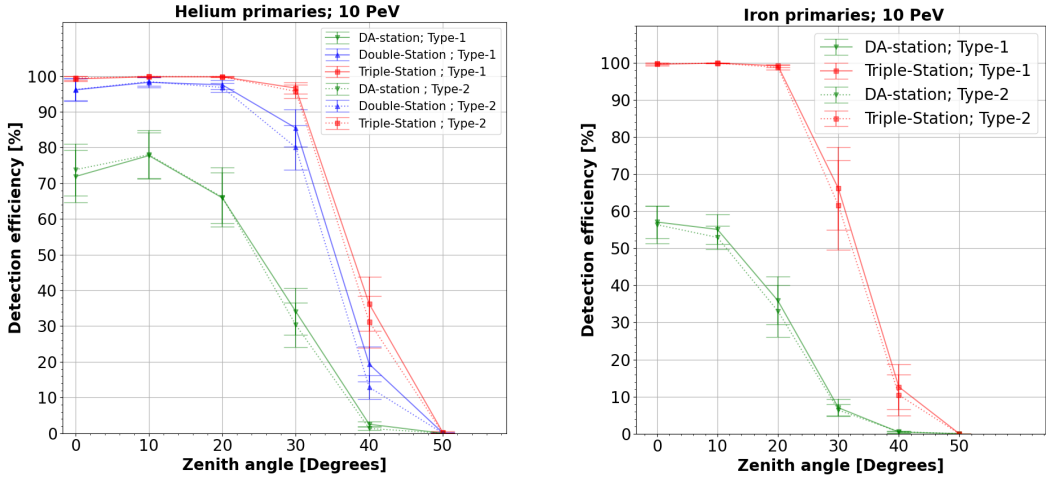


**Figure 7:** Left Profile shows variation of the detection efficiency with increasing number of antennas, for helium primaries. Right Profile presents variation of the detection efficiency with increasing number of antennas, for iron primaries. Notations are same as Figure 6.

value is in the range 24-32 m, preferably 24 m. A typical layout of the TS-array is presented on the right profile of Figure 5. We have also compared the performance of the DA-stations, the DS-array, and the TS-array, for varying zenith angle and different primaries in Figure 6 and Figure 7. With 63 antennas, the detection efficiency hits nearly 100% till 30° zenith angle for proton and helium primaries. For iron primaries, the detection efficiency is 100% till 20° zenith angle. The detection threshold is  $4\sigma$  where  $\sigma$  is defined as the RMS of the noise portion in the trace.

### 3.3 Optimal band of operation

We have also investigated the dependence on the frequency band of operation. Below 100 MHz, the galactic background noise is overwhelming. Hence, the SNR is expected to be higher at higher frequencies [8]. We have compared the BF-performance of the arrays in two different frequency bands, namely the 100-200 MHz and 150-250 MHz frequency bands. We have observed that the BF-performance is significantly better in the 100-200 MHz band, for the designed array. A typical example is presented in Figure 8, where we can clearly note that the SNR and the detection efficiency are significantly higher in the 100-200 MHz frequency band. This also indicates that the designed array is optimally functional in the 100-200 MHz frequency band.

## 4. Conclusions

We have presented our analysis on the design and optimization of a radio-array for the radio-extension of the GRAPES-3 experiment. We have shown that the DA-geometry produces better SNR and detection efficiency. Hence, it is promoted as the base-array geometry, the optimal range for  $d_{ST}$  is in 8-16 m, the optimal range of  $D_{ST}$  is in 24-32 m, the optimal band of operation is 100-200 MHz. We have demonstrated that the detection efficiency peaks for the TS-arrays with 63 antennas. For proton and helium primaries the detection efficiency is nearly 100% till 30° zenith angle and

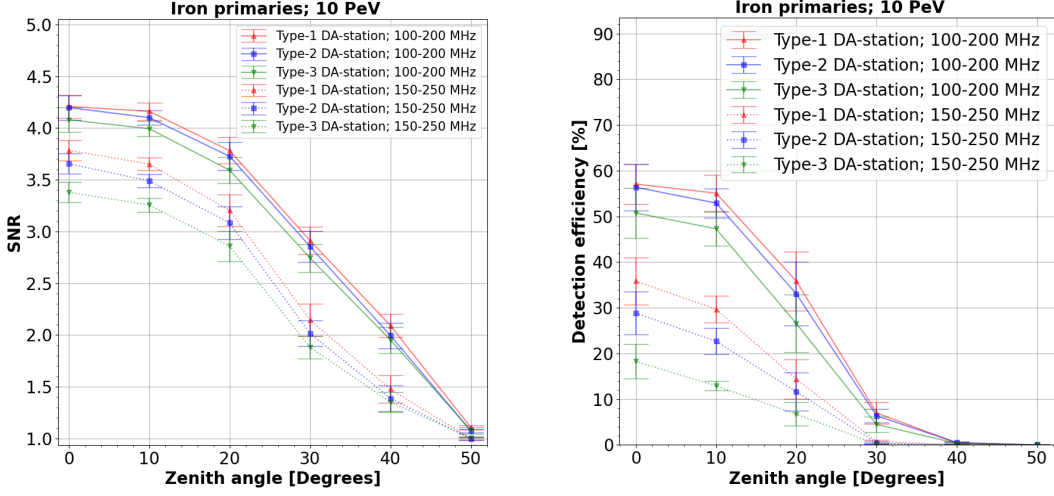


**Figure 8:** The angular variation of the SNR and triggering efficiency in two different frequency bands have been presented here. Type-1 (in Red), Type-2 (in Blue) and Type-3 (in Green) DA-stations have been compared. The solid lines represent 100-200 MHz frequency band and the dashed lines represent 150-250 MHz frequency band.

for the iron primaries the detection efficiency is 100% till 20° zenith angle at the primary energy 10 PeV.

## Acknowledgement

I express my gratitude to the LOFAR/SKA High Energy Cosmic Ray Group for their valuable suggestions on my work. Throughout this work, many of my friends, seniors, and colleagues have helped in various aspects, so I would like to thank them all sincerely.

## References

- [1] H. Schoorlemmer, W. R. Carvalho Jr *Eur. Phys. J. C* 81: 1120 (2021).
- [2] F. Schlüter and T. Huege *JINST* 16 P07048 (2021).
- [3] T. Huege, M. Ludwig and C.W. James *AIP Conf. Proc.* 1535, 128 (2013).
- [4] C. Glaser et al. *Eur. Phys. J. C* 79, 464 (2019).
- [5] E. de Lera Acedo et al. *Exp. Astron.* 39:567–594 (2015).
- [6] Oliveira-Costa et al. *Mon. Not. R. Astron. Soc.* 388, 247–260 (2008).
- [7] H. Zheng et al. *Mon. Not. R. Astron. Soc.* 464, 3486 (2017) .
- [8] V. Balagopal et al. *Eur. Phys. J. C* 78, 111 (2018).
- [9] T. Huege and D. Besson *Prog. Theory. Exp. Phys.* 2017, 12A106 (2017).